Journal of Hydroscience and Hydraulic Engineering
Vol. 20, No.2 November, 2002, 187-196

FLOW AND SPREADING MECHANISM OF THREE-DIMENSIONAL NEGATIVE BUOYANT SURFACE JETS RELEASED ON A SLOPING BOTTOM

By

Masanori Nakai

Department of Civil and Environmental Engineering, Tokyo Denki University
Hatoyama-machi, Hiki-gun, Saitama, 350-0394, Japan,

Masamitsu Arita

Department of Civil and Environmental Engineering, Tokyo Denki University
Hatoyama-machi, Hiki-gun, Saitama, 350-0394, Japan

and

Yasunori Tahara

Department of Civil and Environmental Engineering, Tokyo Denki University
Hatoyama-machi, Hiki-gun, Saitama, 350-0394, Japan

SYNOPSIS

This study deals with the behavior of three-dimensional negative buoyant surface jets released on a sloping bottom. Flow visualization and exhaustive thermometry were carried out to investigate the streamwise variations of the flow and spreading characteristics. The jet gradually separates into surface and bottom flows, being inserted an intermediate layer between them, after passing the jet-like region. In succession, the surface flow momentarily plunges, re-rises and re-attaches on the water surface, and then, exhibits great lateral spreading. Finally, it completely plunges down and re-coalesces in the intermediate and bottom layers. This behavior is peculiar in the three-dimensional case and plays an essential role in the flow and spreading.

INTRODUCTION

Negative buoyant surface jets discharged on a sloping bottom are important in hydraulics and are associated with various environmental problems. This phenomenon is often observed in lakes, reservoirs and seas, such as inflow of river water with a lot of suspended sand grains into reservoirs, and cool water release from power plants to coastal seas. Therefore, many studies concerning this phenomenon have been done for the two-dimensional and quasi-three-dimensional cases (Turner (14), Fukuoka, Fukushima and Nakamura (6), Akiyama and Stefan (1), Johnson et al. (10), Stefan and Johnson (12), Fukushima (7), Ishikawa, Nagao and Nagashima (9), Arita and Tsukahara (4), Lee and Yu (11)).

Although the full three-dimensional case in which flow spreading appears also in the lateral direction is common in actual fields, only a few researchers have treated this case (Hauenstein and Dracos (8), Tsihrintzis and Alavian (13), Fleenor and Schladow (5)). The authors also experimentally studied the full three-dimensional case and attempted to clarify its flow mechanism (Arita et al. (3), Arita, Nakai and Umemoto (2)). They pointed out the existence of a peculiar flow mechanism being based on their detailed laboratory experiments. In this paper, the authors summarize their experimental results including additional data and discuss the details of the flow mechanism.

OUTLINE OF THE PHENOMENON

Fig.1 shows an outline of the full three-dimensional flow and a definition sketch. A full three-dimensional negative buoyant surface jet with an initial densimetric Froude number F_o discharges on a sloping bottom of a slope S and plunges into a bottom layer at a distance L_p from an outlet. After that, the flow runs down along a sloping bottom as a three-dimensional buoyant inclined jet. Herein, $F_o = U_o/\{(\Delta \rho_o/\rho_a) gH_o\}^{1/2}$; U_o = initial velocity of the jet ; $\Delta \rho_o = \rho_o - \rho_a$ = initial density difference ; ρ_o = initial density of the jet ; ρ_a = density of ambient water ; H_o = initial flow depth ; and g = gravitational acceleration (see Fig.1). In the following, 'the full three-dimensional negative buoyant surface jet released on a sloping bottom' will simply be called 'the jet'.

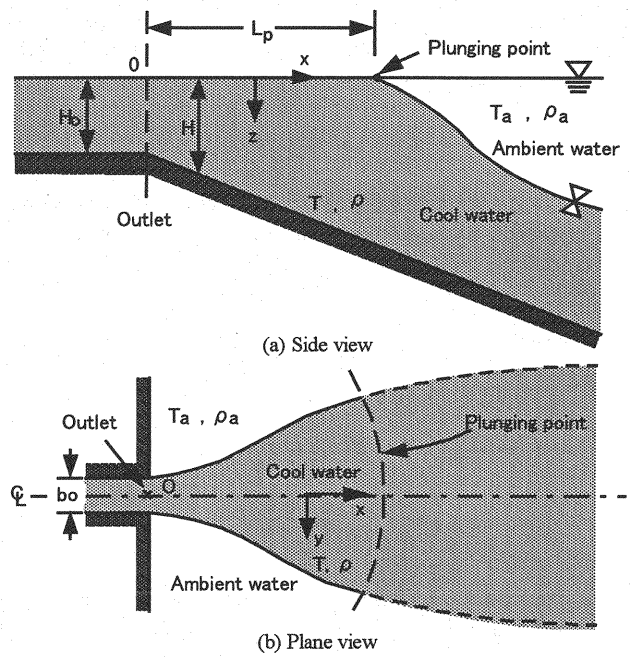

Fig.1 An outline of the flow and a definition sketch.

EXPERIMENT

A water tank of 6.0(m) long, 2.5(m) wide and 0.6(m) deep was used in this experiment. A channel of 5.0(cm) wide for jet release was connected to the water tank, and an acrylic plate for a sloping bottom was set in the water tank. A multi-port pipe for water draining was installed in the downstream side of the water tank to keep a constant water depth.

In the experiment, cool water jets of 5.0(cm) ($=b_o$) wide and 4.0(cm) ($=H_o$) deep were released from the channel into slightly warm water in the water tank. The flow patterns in longitudinal-sections and cross-sections were visualized, using a slit beam, by fluorescent dye with Al flakes and were photographed by means of a video camera. In addition, exhaustive thermometry was carried out, using many thermistor-type thermometers, to obtain time-averaged temperature distributions in the both sections.

The experimental conditions were as follows. The flow rate Q and the temperature difference at an outlet ΔT_o were changed in the ranges of 0.15～0.30(ℓ/s) and of 4.0～6.0(℃) respectively, and the bottom slope S was set to 1/5, 1/10 and 1/40. Consequently, the values of the initial densimetric Froude number F_o were in the range of $2<F_o<13$.

EXPERIMENTAL RESULTS

In this paper, the focus of discussion is only on one case : F_o = 6.2～6.5 and S =1/5, because various data

were obtained in this case (this case will be called 'the typical case'), and comparisons with other cases are carried out. In the following, experimental results without designation belong to the typical case.

Fig.2 shows the visualized photographs in three cross-sections of the jet in a steady state. Herein, x expresses the distance from an outlet. In Fig.2(a) (x/H_o=1.25 : near an outlet), the spreading width is almost uniform in the vertical direction. In Fig.2(b) (x/H_o=5.0), the bottom layer widens slightly and weak constriction emerges in the intermediate layer. In Fig.2(c) (x/H_o=10.0 : near a plunging point), spreading develops in the surface and bottom layers and intense constriction appears in the intermediate layer. The extensive spreading in the surface layer, which was first recognized in our experiment (Arita, Nakai and Umemoto (2)), suggests rising up of the jet against gravity force. The flow characteristics in the surface, intermediate and bottom layers are quite different from one another, and this fact is significant and will be discussed later. Herein, white-colored regions widely exist on the slope in Fig.2(a) and (b), it is thought that the regions are images of cool water masses, visualized by a slit beam, remaining near the bottom of the tank after flowing down on the slope.

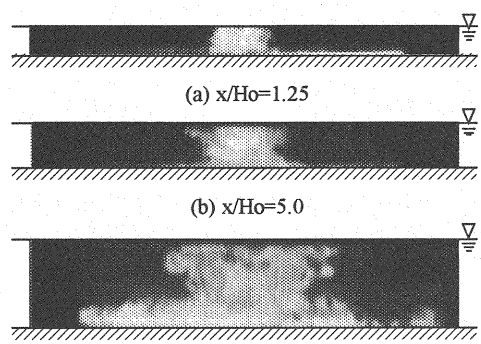

Fig.2 The cross-sectional spreading visualized by dye with Al flakes (F_o = 6.5 and S = 1/5).

Fig.3 depicts the continuously visualized photographs on the stream-axis in the longitudinal- section (time intervals of the neighboring pictures are about 0.5(s)). The surface flow momentarily plunges in Fig3.(a), re-rises and re-attaches on the water surface in Fig.3(b) – (d), and returns to its original shape in Fig.3(e) (same as Fig.3(a)). From a detailed observation, it was found that this consecutive motion repeats at an almost same location with intermittence. The surface flow completely plunges into the bottom layer immediately after the re-attachment. In addition, another picture for a different case (F_o = 2.9 and S =1/5) is shown in Fig.8(a), the re-rising and re-attachment of the surface flow can be clearly recognized from this picture.

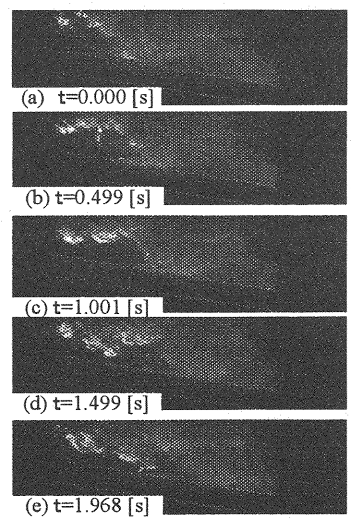

Fig.3 The flow behavior on the stream-axis in the longitudinal-section visualized by dye with Al flakes (F_o = 6.2 and S = 1/5).

In the typical case and similar cases, F_o is small or medium and S is large, and the re-rising and re-attachment appear only once in the flow-down process. On the other hand, in cases with large F_o and small S, it can be considered that this phenomenon repeats several times in the flow-down process. The mechanism of the consecutive motion and its effects will be discussed later.

We attempted to analyze the flow characteristics of the jet using time series data of temperature. The two parameters adopted are as follows :

$$R_c(\tau)=\frac{\overline{\{T_1(t)-\overline{T_1}\}\{T_2(t+\tau)-\overline{T_2}\}}}{\sqrt{\overline{\{T_1(t)-\overline{T_1}\}^2}}\sqrt{\overline{\{T_2(t)-\overline{T_2}\}^2}}} \tag{1}$$

$$\alpha=\frac{\sqrt{\overline{\Delta T'^2}}}{\overline{\Delta T}} \tag{2}$$

where, $R_c(\tau)$ = cross-correlation factor ; α = turbulence intensity ; $\Delta T = T_a - T$; T_a = ambient water temperature ; T = local water temperature in the jet ; $\Delta T'$ = turbulent component of ΔT ; t = time ; and τ = lag time. In addition, over-bars denote a time-averaging operation and subscripts 1, 2 indicate two vertically neighboring points with a distance of 1.0(cm) ; points 1 and 2 are lower and upper points respectively. $R_c(\tau)$ denotes the degree of the correlation between points 1 and 2. Large values of $R_c(\tau)$ mean strong correlation, and $\tau>0$ and $\tau<0$ express upward and downward flows between points 1 and 2 respectively. Sampling times of the temperature data are about 30(s) and data intervals are about 0.1(s).

Fig.4 shows the distribution of the vertical flows on the stream-axis in the longitudinal-section. In this figure, the numerical values express the lag time $\tau=\tau_m$ at which $R_c(\tau)$ exhibits maximum values, and the arrows denote directions of the vertical flows (if $R_c(\tau_m)<0.5$, the numerical values of τ_m are deleted in this figure. In these cases, the degree of the correlation between points 1 and 2 is thought to be small). Small values of $|\tau_m|$ indicate a strong upward or downward flow, and its flow velocity can be approximately expressed by $1/|\tau_m|$ (cm/s).

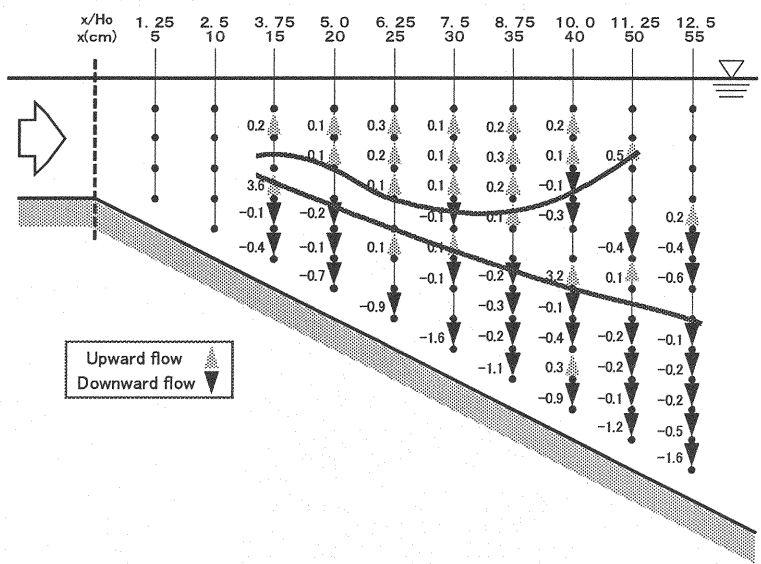

Fig.4 The distributions of the lag time τ_m, the upward and downward flows on the stream-axis in the longitudinal-section (F_o = 6.2 and S = 1/5). The solid lines indicate an outline of the boundaries between the neighboring fluid layers.

Let us discuss the characteristics of the vertical flows, according to Fig.4, by dividing the total flow field into three ranges in the streamwise direction. In the range of $x/H_o \leqq 2.50$: near an outlet, the values of $R_c(\tau_m)$

are less than 0.5 all over the field, so the degree of the correlation between vertically neighboring points is small and the vertical flows are negligibly weak. In the range of $3.75 \leqq x/H_o \leqq 8.75$, the values of $|\tau_m|$ are less than 0.3(s) at a lot of points except near the bottom. Upward and downward flows occur in the surface and bottom layers respectively, and the jet separates in the vertical direction. The intermediate layer in which vertical velocity is almost zero exists between the both flows. Furthermore, very slow downward flows are observed near the bottom. In the range of $x/H_o \geqq 10.00$: around a plunging point, downward flows dominate all over the bottom layer and appear also in the surface and intermediate layers. In addition, the thickness of the intermediate layer largely increases. These findings suggest that the surface flow plunges and re-coalesces in the intermediate and bottom layers, and that the re-coalesced jet runs down along a sloping bottom as an inclined negative buoyant jet.

Fig.5 indicates the distribution of the turbulence intensity α on the stream-axis in the longitudinal-section. In the bottom layer, the relatively small values of α are observed, which means that a stable flow is produced along a sloping bottom. While, the values of α in the surface layer are greater than those in the bottom layer, in particular, they tend to be extremely large around the re-attachment point ($8.75 \leqq x/H_o \leqq 12.5$), due to the consecutive motion ; in other words, the momentary plunging, re-rising and re-attachment.

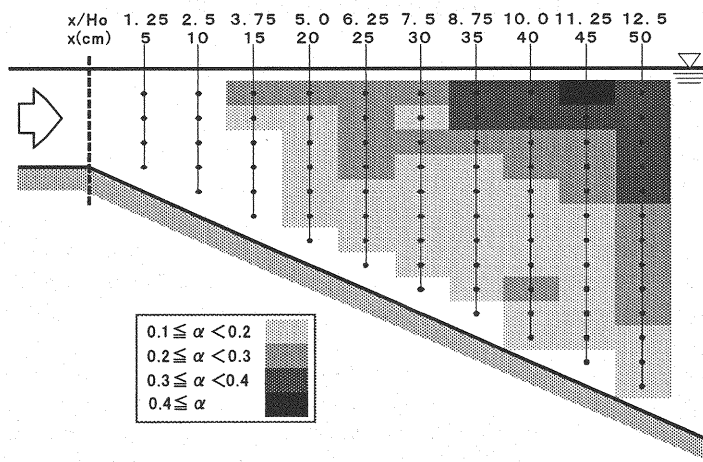

Fig.5 The distribution of the turbulence intensity α on the stream-axis in the longitudinal-section (F_o = 6.2 and S = 1/5).

SPREADING CHARACTERISTICS

Herein, the spreading of the jet is discussed in consideration of the fact that the total flow layer can be divided into surface, intermediate and bottom layers.

Fig.6 summarizes the spreading process of the jet. The jet behaves like a non-buoyant jet near an outlet and its spreading is almost uniform in the vertical direction (cross-section①). Horizontal entrainment of ambient water is strongly generated through the both side edges of the jet. Fig.2(a) and the range of $x/H_o \leqq 2.50$ in Fig.4 correspond to this region which is called 'the jet-like region'. The jet loses inertia force with running down and its characteristic changes into a transient state. In the transient region, the jet gradually separates into surface and bottom flows being inserted an intermediate layer between them. Spreading due to the effect of gravity develops in the bottom layer, and furthermore, a downward flow originates from the intermediate layer to the bottom layer. Consequently, weak constriction emerges in the intermediate layer (cross-section②). In addition, an upward flow occurs in the surface layer simultaneously with the downward flow, and this is also a cause of the weak constriction. Fig.2(b) and the range of $3.75 \leqq x/H_o \leqq 6.25$ in Fig.4 correspond to this region. Subsequently, the weak constriction disappears and the cross-section changes to be bell-shaped, and the surface flow momentarily plunges at the same time (cross-section③). The point of x/H_o=7.50 in Fig.4 is thought to belong to this region.

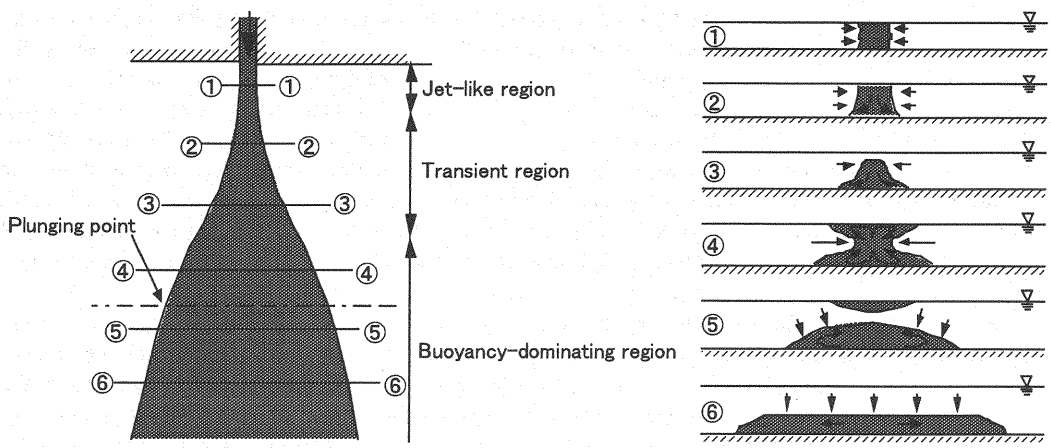

(a) Plane view (b) Cross-sectional views

Fig. 6 The streamwise variation of the spreading of the jet.

Then, the jet enters 'the buoyancy-dominating region' through the transient region. The bottom layer greatly expands and the surface flow re-rises and re-attaches on the water surface against gravity force. The surface layer extensively spreads and intense constriction occurs in the intermediate layer just after the re-attachment (cross-section ④). Fig.2(c) and the range of $8.75 \leqq x/H_o \leqq 10.00$ in Fig.4 correspond to this region. After that, the surface flow reaches a plunging point and completely plunges down. On the other hand, the bottom flow runs down along a sloping bottom with the intermediate layer. Some water masses in the surface layer, however, go over the plunging point and remain near the water surface (cross-section⑤). The water masses gradually diffuse into ambient water and disappear. The surface flow finally re-coalesces in the intermediate and bottom layers after the complete plunging, and the re-coalesced jet runs down along a sloping bottom as an inclined buoyant jet (cross-section⑥).

The three regions mentioned above, that is, the jet-like, transient and buoyancy-dominating regions are thought to be divided by the over-all densimetric Froude number F_d defined by local quantities. The jet belongs to the jet-like region near an outlet and enters the buoyancy-dominating region through the transient region with a decrease in F_d in the flow-down process. Accordingly, the jet-like region is extended to a far field in cases of large F_o. The extension of the jet-like region appears also in cases of small S, because the inertial force in the jet slowly decreases with running down due to the suppression of vertical spreading.

The experimental results to verify the accuracy of the above description are shown in Fig.7. This figure represents the distributions of the time-averaged dimensionless temperature difference $\Delta T/\Delta T_0$ in cross-sections in cases of F_o = 3.1, 6.3 and 12.1. In these cases, S and x/H_o are fixed to 1/10 and 5.0 respectively, and sampling times of the temperature data are about 30(s). The cross-sectional shape of the jet is almost rectangular in Fig.7(a) (F_o = 12.1). In Fig.7(b) (F_o = 6.3) and (c) (F_o = 3.1), in contrast, weak and intense constriction is generated in the intermediate layer respectively. These results show that Fig.7(a), (b) and (c) correspond to cross-sections①, ②and ④in Fig.6 and belong to the jet-like, transient and buoyancy-dominating regions respectively and verify that the transition of the jet depends on F_o as mentioned above (details of the experimental results concerning Fig.7 can be found in Arita, Nakai and Umemoto (2)).

MECHANISM OF RE-RISING AND RE-ATTACHMENT

Let us discuss the mechanism of the re-rising and re-attachment of the surface flow. Herein, we consider the moment when the surface flow plunges slightly, as shown in Fig.9 (corresponding to cross-section③ in Fig.6), and propose two hypotheses on this mechanism being based on the above experimental results.

One of the hypotheses is as follows (see Fig.8). At the moment, the surface flow downward entrains the ambient water just on it. Since the ambient water region between the water surface and the upper edge of the jet is very narrow, entrainment velocity will be large and pressure will drop in this region. Then, the surface flow can re-rise and re-attach on the water surface due to so-called the Coanda effect.

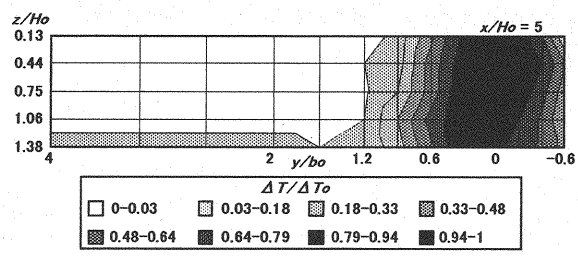

(a) Fo=12.3

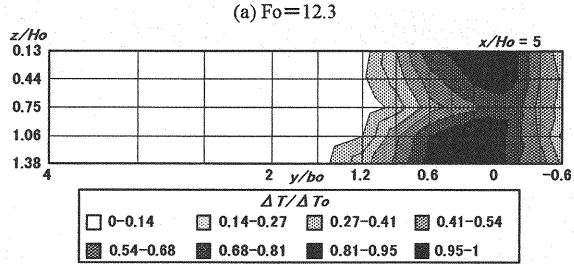

(b) Fo=6.3

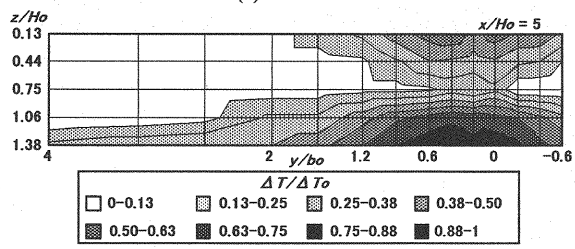

(c) Fo=3.1

Fig.7 The variation of the cross-sectional shape of the jet with F_o (S = 1/10 and x/H_o = 5.0).

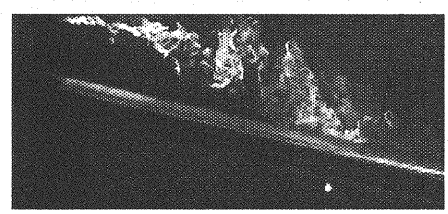

(a) Re-rising and re-attachment of the surface flow (Fo=2.9, S=1/5)

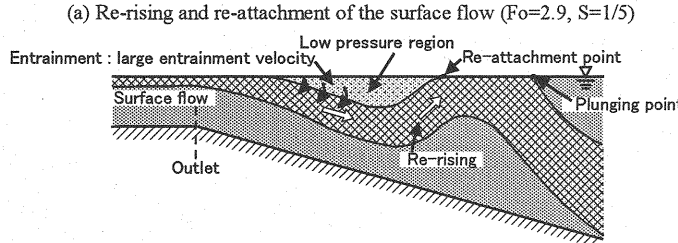

(b) Explanation of the Coanda effect

Fig.8 The visualized flow pattern on the stream-axis in the longitudinal-section and its sketch.

The other hypothesis is associated with eddy-induced velocity. It is suggested, by the two special features : the separation of the total flow layer and the weak constriction in the intermediate layer (see Fig.2(b) and Fig.4), that two pairs of longitudinal eddies are formed both in the surface and bottom layers (see Fig.9). In the bottom layer, a density current with a Karman head, which is composed of intruding and reverse flows, is generated in the spanwise direction, and a downward flow is also produced on the stream-axis as previously mentioned. They form a pair of eddies in the bottom layer. In addition, another pair of eddies will be driven in

the surface layer as compensation for those in the bottom layer. These two pairs of eddies play an important role in the flow and spreading of the jet.

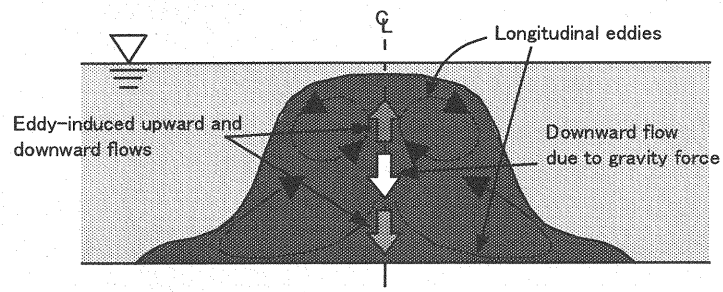

Fig.9 A sketch of the flow pattern in the cross-section at momentary plunging (the transient region).

Herein, the effects of the longitudinal eddies are discussed at the moment shown in Fig.8. The size of the paired eddies in the surface layer will be small by the momentary plunging, and their vorticity increases and the distance between the eddies decreases. Then, the upward flow on the stream-axis strengthens due to an increase in the eddy-induced velocity, which can trigger off the re-rising and re-attachment of the surface flow. In the bottom layer, on the other hand, the downward flow on the stream-axis is accelerated by an addition of the eddy-induced flow to the effect of gravity.

The mechanism of the re-rising and re-attachment of the surface flow can be summarized as follows. The surface flow re-rises and re-attaches on the water surface, after the momentary plunging, due to the Coanda effect as well as an increase in the eddy-induced velocity. The strong upward flow due to the both effects makes not only the re-rising of the surface flow but also the great lateral spreading in the surface layer after the re-attachment.

CONCLUSION

In this study, the flow and spreading mechanism of full three-dimensional negative buoyant surface jets released on a sloping bottom was experimentally investigated. The conclusion obtained is as follows.

In the transient region, the jet gradually separates into surface and bottom flows being inserted an intermediate layer between them, and weak constriction appears in the intermediate layer. After that, the surface flow momentarily plunges, re-rises and re-attaches on the water surface before complete plunging. The consecutive motion, which is peculiar in the three-dimensional case, is caused by the Coanda effect and by an increase in the eddy-induced velocity. However, the degree of these effects to the phenomenon is unknown, and we must determine it in our future studies.

ACKNOWLEDGEMENT

We would like to express our special thanks to Prof. Jirka, University of Karlsruhe for his valuable comments. He observed constriction in a cross-section of a three-dimensional non-buoyant jet with a shallow depth and attributed its origin to a secondary flow produced in the cross-section. We think that a similar secondary flow may be a cause of the constriction observed in our experiment. Additional studies in regard of this matter need to be carried out.

REFERENCES

1. Akiyama, J. and Stefan, H.G. : Plunging flow into a reservoir : Theory, J. Hydr. Engrg., ASCE, Vol.110, No.4, pp.484-499, 1984.
2. Arita, M., Nakai, M. and Umemoto, J. : Flow and spreading of three-dimensional negatively buoyant surface jets discharged on a sloping bottom, Proc. 5th Int. Sym. on Stratified Flows, pp.1099-1104, 2000.
3. Arita, M., Nakai, M., Watanabe, T. and Umemoto, J. : An experimental study on three-dimensional egatively buoyant surface jets discharged on a slopping bottom, Proc. Hydr. Engrg., JSCE, Vol.42, pp.535-540, 1998

(in Japanese).
4. Arita, M. and Tsukahara, C. : Experimental study on the plunging conditions of the negative surface buoyant jet, J. Japan Soc. Fluid Mech., Vol.15, No.5, pp.409-416, 1996 (in Japanese).
5. Fleenor, W.E. and Schladow, S.G. : Mixing in the plunge zone of lake inflows, Proc. 5th Int. Sym. on Stratified Flows, pp.307-312, 2000.
6. Fukuoka, S., Fukushima, Y. and Nakamura, K. : Study on the plunge depth and interface form of density currents in a two-dimensional reservoir, Proc. JSCE, No.302, pp.55-65, 1980 (in Japanese).
7. Fukushima, Y. : Analysis of inclined wall plume by turbulence model, J. Hydr. and Sanitary Engrg., JSCE, No.399, pp.65-74, 1988 (in Japanese).
8. Hauenstein, W. and Dracos, T. : Investigation of plunging density currents generated by inflows in lakes, J. Hydr. Res., Vol.22, No.3, pp.157-179, 1984.
9. Ishikawa, T., Nagao, M. and Nagashima, S. : Entrainment coefficient of saline plume on the slope of lake Ogawara, Proc. Hydr. Engrg., Vol.40, pp.595-600, 1996 (in Japanese).
10. Johnson, T.R. , Farrell, G.J. , Ellis.C.R. and Stefan, H.G. : Negatively buoyant flow in a diverging channel. I : Flow regimes, J. Hydr. Engrg., ASCE, Vol.113, No.6, pp.716-730, 1987.
11. Lee, H.Y. and Yu, W.S. : Experimental study of reservoir turbidity current, J. Hydr. Engrg., ASCE, Vol.123, No.6, pp.520-528, 1997.
12. Stefan, H.G. and Johnson, T.R. : Negatively buoyant flow in a diverging channel. III : Onset of underflow, J. Hydr. Engrg., ASCE, Vol.115, No.4, pp.423-436, 1989.
13. Tsihrintzis, V.A. and Alavian, V. : Spreading of three-dimensional inclined gravity plumes, J. Hydr. Res., Vol.34, No.5, pp.695-710, 1996.
14. Turner, J.S. : Buoyancy Effects in Fluids, Cambridge Univ. Press, pp.178-186, 1973.

APPENDIX – NOTATION

The following symbols are used in this paper :

b_o	= width of a channel for jet release ;
F_d	= over-all densimetric Froude number defined by local quantities ;
$F_o = U_o/\{(\Delta \rho_o/\rho_a)gH_o\}^{1/2}$	= initial densimetric Froude number ;
g	= gravitational acceleration ;
H_o	= initial depth of the jet ;
L_p	= distance between an outlet and a plunging point ;
Q	= flow rate of the jet at an outlet ;
$R_c(\tau)$	= cross-correlation factor with respect to water temperature ;
S	= slope of a bottom ;
t	= time ;
T	= local water temperature in the jet ;
T_1, T_2	= water temperatures at vertically neighboring points with a distance of 1.0(cm) in the jet ;
T_a	= ambient water temperature ;
U_o	= initial velocity of the jet ;
x	= distance from an outlet ;
α	= turbulence intensity with respect to water temperature ;

$\Delta T = T_a - T$	= local temperature difference ;
$\Delta T'$	= turbulent component of ΔT ;
ΔT_o	= initial temperature difference ;
$\Delta \rho_o = \rho_o - \rho_a$	= initial density difference ;
ρ_a	= density of ambient water ;
ρ_o	= initial density of the jet ;
τ	= lag time ;
τ_m	= lag time at which $R_c(\tau)$ exhibits maximum values ; and
$\overline{\ }$ (over-bar)	= time-averaging operation.

(Received May 17, 2002 ; revised September 10, 2002)